SAGE-Hindawi Access to Research
International Journal of Electrochemistry
Volume 2011, Article ID 173462, 8 pages
doi:10.4061/2011/173462

Research Article

Electrochemical Study on Corrosion Inhibition of Copper in Hydrochloric Acid Medium and the Rotating Ring-Disc Voltammetry for Studying the Dissolution

A. K. Satpati and A. V. R. Reddy

Analytical Chemistry Division, Bhabha Atomic Research Centre, Mumbai 400085, India

Correspondence should be addressed to A. K. Satpati, asatpati@barc.gov.in

Received 5 July 2010; Revised 22 October 2010; Accepted 3 January 2011

Academic Editor: Mohamed Mohamedi

Dissolution characteristics of copper in hydrochloric acid medium and the effect of 4-amino 1,2,4-triazole (ATA) on the corrosion process have been studied using conventional electrochemical techniques and rotating ring-disc electrodes (RRDEs). Corrosion potential (E_{corr}) and corrosion current density (I_{corr}) were obtained by Tafel extrapolation methods. Charge transfer resistance (R_{ct}) and double-layer capacitance (C_{dl}) were obtained from the electrochemical impedance spectroscopy (EIS). ATA was shown to be an effective inhibitor for the copper-corrosion inhibition in acid medium. The corrosion rate was retarded in presence of inhibitors mainly because of the adsorption of the inhibitor on the electrode surface. Adsorption of the inhibitor on the metal surface was found to follow the Langmuir adsorption isotherm. Standard free energy change of the adsorption process (ΔG^0_{ad}) was calculated to be -54.3 kJ mol^{-1}; such a large negative value of ΔG^0_{ad} suggests the prescence of a chemisorption process.

1. Introduction

Copper and its alloys are widely used in heating and cooling devices due to their high thermal conductivity, good corrosion resistance, and mechanical workability. Such devices are cleaned by acid pickling process using hydrochloric acid solution. It is important to reduce the destructive effect of hydrochloric acid on the devices during the cleaning process. Copper is a relatively noble metal, and the hydrogen evolution is not a usual part of the corrosion process. In nuclear industry, copper alloys are used in condensers where the steam after turning the turbine is required to be cooled. Sea water and fresh water are used for the cooling purpose depending on the location of the plant. Organic surfactants are used as corrosion inhibitors with aqueous solution of acid to reduce the destructive effect of acids. There are studies where benzotriazole has been used as the inhibitor in acid corrosion of copper and steel [1–5]. Heakal and Haruyama [6] and Chialvo et al. [7] have used benzotriazole as the corrosion inhibitor in NaCl solution; in the latter case, kinetics of Cu passivation were discussed. In the present scenario, use of substituted derivatives of triazoles and imidazoles for effective use as an inhibitor is the topic of interest [8–18]. In a part of our study, benzotriazole was used as the inhibitor for studying the acid corrosion of stainless steel [19, 20]. Srhiri et al. have used derivatives of ATA for corrosion inhibition of Cu and Cu-Zn alloys [21, 22]. In corrosion the inhibition process, the dissolution pathways of the materials under protection are very important to know. In some reports [23, 24], dissolution pathways of copper have been studied using transient electrochemical techniques. In the present investigation, dissolution process of copper in acidic solution was studied using rotating ring-disc voltammetry along with the conventional polarization method. The organic molecule 4-amino 1,2,4-triazole (ATA) was used as the inhibitor, and the mechanism of its interaction with copper was studied. In combination with polarization experiments, current transient behaviour of copper dissolution and passivation were studied using electrochemical impedance spectroscopy and electrochemical noise measurements. Electrochemical

noise, which provides finer details of the corrosion process, was used in the present investigation in order to obtain useful statistical information about the corrosion inhibition process.

2. Experimental

High-purity copper metal was cut in the form of electrode from a copper rod. It was polished mechanically with emery papers of up to 600 grit and then with diamond paste of a 5-μm size. After polishing, the electrode surface was degreased with acetone, then washed with distilled water and dried under dry air flow. This electrode, with an exposed surface area of 0.5 cm^2, was then dipped into the corrosion test solution of 0.5 M HCl, which was deaerated by purging with high-purity nitrogen gas for 900 seconds. The samples were allowed to stabilize the open circuit potential (OCP) for half an hour before electrochemical scanning. This electrode was then used as the working electrode with Pt foil as the counter and saturated calomel as the reference electrode. Potentiodynamic polarization was carried out by scanning the potential from −0.4 V to 0.1 V (SCE) at a scan rate of 0.5 mV s^{-1}. Polarization experiments were carried out using a potentiostat from Eco Chemie BV, The Netherlands, Autolab 100, and plots were analyzed with Autolab software. AC impedance investigations were carried out using the same Potentiostat Autolab 100 with an attached frequency response analyzer module (FRA). EIS was employed by applying the sinusoidal voltage pulse of amplitude of 5 mV and in the frequency range of 10 kHz to 45 mHz. Electrochemical noise experiments were carried out with electrochemical noise module (ECN) fitted with the potentiostat at open circuit condition.

3. Results and Discussion

3.1. Polarization Study. Polarization plots were obtained for the copper electrodes in a 0.5-M HCl solution in presence and in absence of different concentrations of inhibitor (cf. Figure 1). A peak at −0.12 V was observed, which is possibly due to the formation of an insoluble product formed by the oxidation of copper. After a certain amount of copper oxidation, the insoluble film on the copper surface was formed due to adsorption of insoluble $CuCl_{ads}$ species which retarded the dissolution process, and the anodic current dropped down. However at very high chloride ion concentration, formation of $CuCl_2^-$ will be facilitated and formation of such peak may not be seen [25]. A detailed investigation of the dissolution was carried out using RRDE voltammetry and the results were discussed in RRDE section (cf. Section 3.3). Both the cathodic current and anodic current density decreased in presence of inhibitors of varying concentrations (Figure 1). Electrochemical parameters namely, corrosion current density (I_{corr}), cathodic and anodic Tafel slopes (B_c and B_a), and corrosion potential (E_{corr}) were calculated from the Tafel extrapolation of the polarization plot and the values were reported in Table 1. Although the corrosion current density decreased in presence of inhibitor, corrosion potential did not change significantly in the presence and absence of the inhibitor. Both the cathodic and anodic Tafel slopes were seen to have changed in the presence of inhibitor. Considering the collective observations on the change in the Tafel slopes, change in current density, and the nature of change of corrosion potentials, the inhibition process appeared to be of mixed type in nature with pronounced effect. The inhibition efficiency (E%) was calculated from the corrosion current density from the following equation:

$$E(\%) = \frac{[I_{\text{uninh}} - I_{\text{inh}}]}{I_{\text{uninh}}} \times 100, \quad (1)$$

where I_{uninh} and I_{inh} are the corrosion current densities in the absence of inhibitor and presence of inhibitor, respectively. The inhibition efficiency of up to 74% was achieved at 10-mM concentration of the ATA.

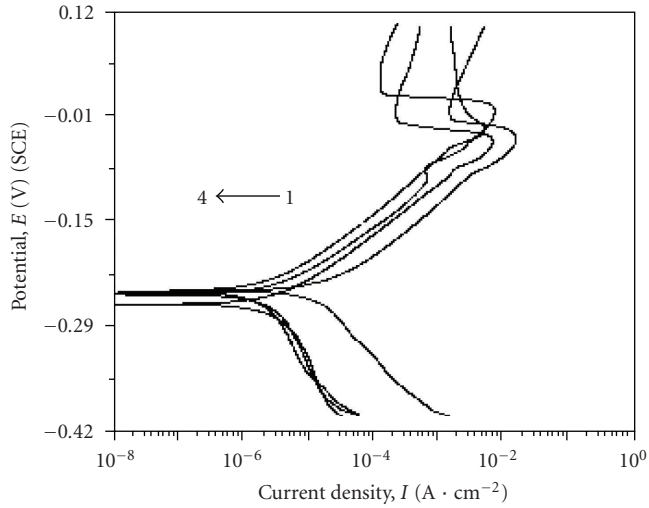

Figure 1: Polarization plots of copper in 0.5-M HCl with and without different concentrations of ATA, without ATA, (1); with 0.1-mM ATA; (2); with 1-mM ATA, (3); with 10-mM ATA, (4).

3.2. Electrochemical Impedance Spectroscopy. Nyquist plot of copper in acidic solutions with and without inhibitor was shown in Figure 2. In the inhibited as well as in the uninhibited solutions the impedance spectra were characterized by two slightly distorted semicircles, one at high-frequency region and the other at low-frequency region. Cu surface was always covered with copper-oxide films formed in the air and also in the aqueous solution. The semicircle at higher frequency was attributed to the oxide layer present on the copper surface. The second semicircle was due to the charge transfer process, contribution of Warburg parameter was significant in the impedance analysis [26–28]. Deviations from the ideal semicircles could be attributed to the inhomogeneities of the surface [29]. Solution resistance (R_s), oxide film resistance (R_{oxide}), charge transfer resistance (R_{ct}) the capacitance values for the oxide film (C_1), and the capacitance (C_2) from the constant phase element (CPE) value were calculated from the analysis of the impedance plots using the equivalent circuit shown in the inset of

Table 1: Results of Tafel slope analysis of the polarization plots at 298 K.

Solution	$i_{corr} \times 10^6$/A cm^{-2}	B_c/mVdec^{-1}	B_a/mVdec^{-1}	E_{corr} /V	η/%
0.5 M HCl	23.4	101	50	−0.245	—
0.5 M HCl + 0.1 mM ATA	8.9	194	60	−0.256	62
0.5 M HCl + 1 mM ATA	7.7	217	65	−0.245	67
0.5 M HCl + 10 mM ATA	5.9	219	64	−0.241	74

Figure 2. The values were tabulated in Table 2. In acid solution without inhibitor, charge transfer resistance and double layer capacitance were obtained to be 300 Ohm cm^2 and 10.3 μF cm^{-2}. Whereas in presence of inhibitor of a 10-mM concentration, the resistance and the capacitance values were 2.0 kOhm cm^2 and 3.5 μF cm^{-2}, respectively. Charge transfer resistance increased with the increase in the inhibitor concentration and at a 10-mM concentration of the inhibitor its magnitude became one-order higher than that in the blank solution. The increase in charge transfer resistance and decrease in the double-layer capacitance with the use of inhibitor have been attributed to the enhanced adsorption of the inhibitor molecule on the metal surface [30]. Increase in the charge transfer resistance resulted in the decrease of metal oxidation reaction at the same potential region. In the present case, due to the electrochemical rough surface instead of ideal capacitive behavior, the constant phase element (CPE) was used to calculate the pure capacitance. The impedance function of CPE (Z_{CPE}) is related to the angular frequency (ω) by the following relation: $Z_{CPE} = Y^{-1}(j\omega)^{-n}$, where Y is a proportionality factor and n is the deviation parameter, which is related to surface roughness [31]. The actual capacitance C as reported in the present case is obtained using the following equation [32–34]:

$$C = \frac{Y\omega^{n-1}}{\sin(n\pi/2)}. \quad (2)$$

Here, the parameter n defines the surface inhomogeneity. The n was varied from 0.85 to 0.92 in different solution conditions measured, which was indicative of the fairly good surface, and the CPE could be deduced to the capacitance using the above-mentioned formula in (2).

3.3. Rotating Ring-Disc Electrode Study. Two sets of experiments with rotating ring-disc electrode (RRDE) were performed with the copper as the disc and Pt as the ring electrode. In the first set, ring electrode was polarized at a cathodic potential (at −0.4 V (SCE)) and the disc electrode was scanned from −0.5 to 0.2 V (SCE) in a 0.2-M HCl solution with and without 0.1-mM BTA inhibitor. The rotation speed was kept at 2000 RPM, and 0.2-M HCl (instead of, 0.5 M used in the polarization experiments) was used in these experiments so as to minimize the copper deposition at the ring electrode. In the second set, the ring potential was anodically polarized (kept at 0.4 V (SCE)) and the disc electrode was scanned in the same way as earlier, from −0.5 to 0.2 V (SCE). Typical plots obtained in both sets of experiments were shown in Figures 3(a) and 3(b). Three peaks obtained in the disc electrode current were designated as "a", "b", and "c" and two peaks obtained in the ring electrode current were designated as "1" and "2" (cf. Figures 3(a) and 3(b)). Three peaks "a", "b" and "c" obtained in the disc electrode polarization were explained on the basis of the formation of different species due to the oxidation of Cu [18, 35–37]

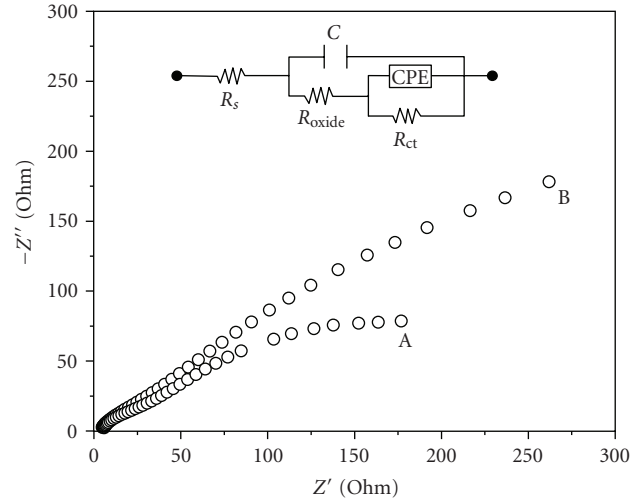

Figure 2: Nyquist plots of copper in 0.5-M HCl, (A) without ATA, (B) with 10 mM of ATA. Inset: the proposed equivalent circuit of the impedance results.

$$Cu + Cl^- \Longleftrightarrow CuCl_{ads} + e \quad (3)$$

$$CuCl_{ads} + Cl^- \Longleftrightarrow CuCl_2{}^-(\text{soluble}) \quad (4)$$

$$CuCl_2{}^-(\text{soluble}) + Cl^- \Longleftrightarrow CuCl_3{}^- + e \quad (5)$$

The peak "a" observed in Figures 3(a) and 3(b) was due to the formation of insoluble $CuCl_{ads}$ species due to reaction (3). However, after formation of the insoluble $CuCl_{ads}$ species, further oxidation of the metal was retarded at that potential region of peak "a". On further anodic polarization of the disc electrode more and more Cl^- ions ingresses in to the passive film and reaction (4) started, which eventually facilitated the forward process of reaction (3) is resulting in peak "b". When the potential was scanned further in the anodic direction, Cu(I) was oxidized to Cu(II) and the passive film was dissolved by forming soluble chloride complex species as represented in reaction (5). A support to the above findings was obtained from the observation of the nature of the ring electrode plot (cf. Figures 3(a) and 3(b)). It was observed

Table 2: Results of capacitance and resistance values from impedance measurements at 298 K.

Solution	R_s/Ohm cm^2	$^*C_1/\mu$F cm^{-2}	R_{oxide}/Ohm cm^2	$^*C_2/\mu$F cm^{-2}	n	R_{ct}/Ohm cm^2
0.5 M HCl	102	1.5	500	10.3	0.85	300
0.5 M HCl + 10 mM ATA	150	0.56	1021	3.5	0.92	2000

$^*C_1$ is obtained from the pure capacitance and C_2 from CPE of the equivalent circuit as shown in the inset of Figure 2.

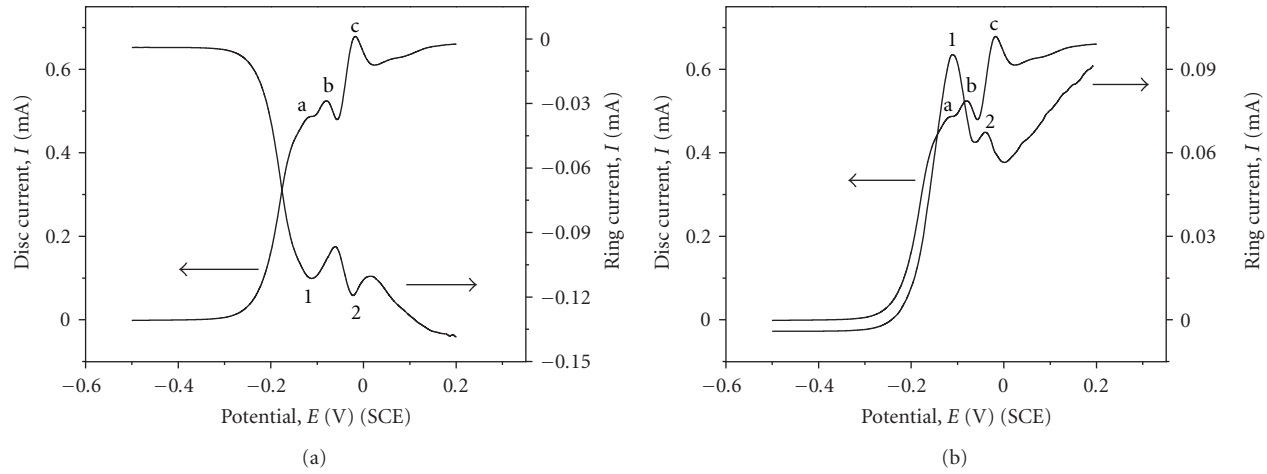

Figure 3: Rotating ring-disc voltammetry plots of copper disc electrode with Pt-ring electrode, (a) the ring electrode was made as a cathode; (b) the ring electrode was made as an anode.

that when the ring electrode was cathodically polarized, it could electroreduce both the Cu(I) and Cu(II) species which come from the disc electrode, and two reduction peaks (cf. Figure 3(a)) were produced. The first peak (peak 1) was due to the reduction of the $CuCl_2^-$ species, and the second peak was due to the reduction of both $CuCl_2^-$ and $CuCl_3^-$ species. On the other hand, when ring electrode was anodically polarized on keeping at 0.4 V (SCE), only the soluble Cu (I) species could be reoxidized and detected (Figure 3(b)). The monovalent copper species was detected in the potential region of peaks 1 and 2 as well as at the pitting region. From the relative current of the two peaks (peaks 1 and 2 of Figures 3(a) and 3(b)), it could be concluded that at higher polarization potential copper preferably dissolved as soluble Cu(II) soluble species and the proportion of formation of soluble Cu(I) species was reduced. The literature's [38–41] reports about the mechanism of dissolution of copper in aqueous solution agreed well with the present observation from RRDE measurements.

3.4. Electrochemical Noise and Surface Morphology Study. Electrochemical noise measurements were carried out with the ECN module fitted with the Autolab potentiostat. Experiments were performed using three identical copper electrodes dipped inside the test solution of 0.5-M HCl with and without 10 mM of ATA. The schematic representation of the electrode setup and connections were explained elsewhere [38]. Noise resistance, R_n, which is equivalent to the charge transfer resistance, R_{ct}, was calculated from the ratio of the standard deviation of the potential noise to the standard deviation of the current noise, that is, $R_n = \sigma_v/\sigma_i$ [42–46]. The calculated values of R_n in the case of acid without inhibitor were 4.0 whereas in the case of ATA with 10-mM concentration it was 4.5. Therefore, the calculated R_n value was observed to be increased while using inhibitor. The noise data were transformed from time domain to the frequency domain and the power spectral density (PSD) plots were obtained. The power spectral density (PSD) is the frequency response of a random or periodic signal. It indicates where the average power is distributed as a function of frequency. The PSD is a deterministic quantity, for certain types of random signals. It is independent of time, which means that statistics of the signal do not change as a function of time. For a random noise signal $N(t)$, the PSD is the average of the squared Fourier transform magnitude over a large time interval

$$\mathrm{PSD}_n(f) = \lim_{t\to\infty} E\left[\frac{1}{2t}\left|\int_{-t}^{t} N(t)e^{-j2\pi f t}dt\right|^2\right], \qquad (6)$$

where $\mathrm{PSD}_n(f)$ is the power spectral density of the time variant noise function $N(t)$, and t is the time interval. In the present experimental setup, current and potential noise were measured as a function of time and Fourier transformation was carried out to get the corresponding PSD plots using the autolab-GPES 4.9 software.

The characteristics frequency (f_n) is generally considered as the parameter, which determines the degree of localized corrosion from electrochemical noise measurement [46]. This "characteristics frequency" is inversely proportional to the potential PSD plot but independent of the current noise. The characteristics frequency was

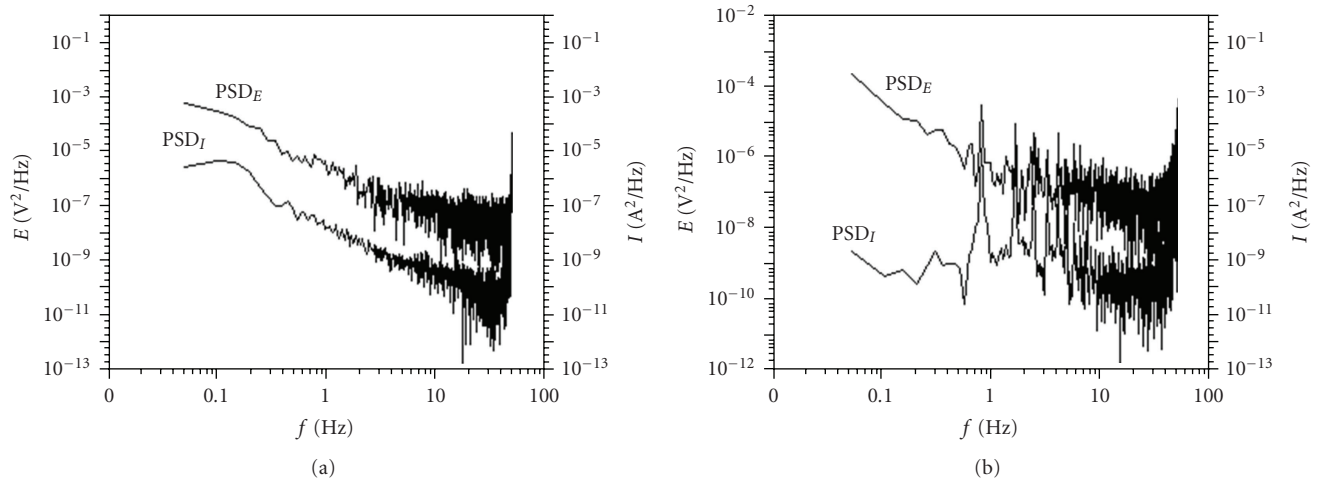

Figure 4: Current and potential noise power spectral density (PSD) plot, (a) copper in 0.5-M HCl, (b) copper in 0.5-M HCl with 10 mM of ATA.

calculated as $f_n = I_{\text{corr}}/q$, where I_{corr} is the corrosion current and q is the charge in the transient. Localized corrosion, which is associated with characteristics frequency, will have higher potential noise amplitude [46]. Comparing the potential PSD plot, Figures 4(a) and 4(b), it could be indicated that PSD$_v$ was nearly one order of magnitude higher in the case of acidic solution without inhibitor compared to that with inhibitor. Therefore, it could be noted from the relative variation of the characteristics frequency that the possibility of localized corrosion was higher in the case of copper in acidic solution without ATA than in presence of ATA.

The slope of the PSD potential (S_V) and the PSD current (S_I) plots are important parameters, which reflect the corrosion performance of copper in the two solutions. S_V and S_I for acid without ATA were calculated to be -1.6 and -1.5, respectively, whereas with 10 mM of ATA the values were -0.65 and -0.45, respectively. The more negative value of the slopes showed the system to be more prone to the formation of metastable pits [44]. Therefore, different analysis of noise data suggested that copper in 0.5-M HCl with 10-mM ATA was less prone to localized corrosion than without ATA, which corroborate the discussions from noise and other studies.

Surface morphology of copper was studied using atomic force microscopy (AFM) measurements using tapping mode of operation. In Figure 5, the AFM topography of copper surface after different conditions were shown. Figure 5(a) represents the well-polished surface before electrochemical polarization. The AFM topograph after solution treatment in 0.5-M HCl for 3 h without inhibitor in open circuit condition is shown in Figure 5(b). The surface roughness was found to be increased due to the corrosion of copper from the surface. Evidence of the localized corrosion was obtained from the roughened surface due to the localized deposits of corrosion product and dips due to formation of pits. The AFM topography in presence of inhibitor 10 mM ATA is shown in Figure 5(c). The surface was found to be well coated with the inhibitor and deposits of corrosion products were found to be less, compared to that without ATA.

3.5. Adsorption Isotherm. The surface coverage (θ) at a given inhibitor concentration was calculated using the following relation:

$$\Theta = \left[\frac{I_{\text{uninh}} - I_{\text{inh}}}{I_{\text{uninh}}}\right], \tag{7}$$

where I_{uninh} and I_{inh} are the corrosion current densities in the absence and presence of inhibitor, respectively. Attempts were made to fit the data to Langmuir or Frumkin adsorption isotherm. It was found that the data were best fitted with the Langmuir adsorption isotherm, according to which the surface coverage (θ) is related to the inhibitor concentration C_{inh} by the following relation:

$$\Theta = \frac{bC_{\text{inh}}}{(1 + bC_{\text{inh}})}. \tag{8}$$

Therefore, the C_{inh}/θ should follow a linear relation with C_{inh}, which was in good agreement with the experimental results as shown in Figure 6. In the present investigation, the adsorption coefficient (b) was found to be very high (1.2×10^6 M^{-1}), signifying strong adsorption process. The standard free energy of adsorption process was calculated using the following equation:

$$b = \frac{1}{55.5}\exp\left(-\frac{\Delta G_a^0}{RT}\right), \tag{9}$$

ΔG_a^0, the standard free energy of adsorption process, was calculated in the present system as -54.3 kJ mol^{-1}. The large negative value of standard free energy of adsorption indicated possible chemical interaction between the delocalized lone pair of electron on the N atom and the π electron cloud with the vacant d orbital of the oxidized copper surface.

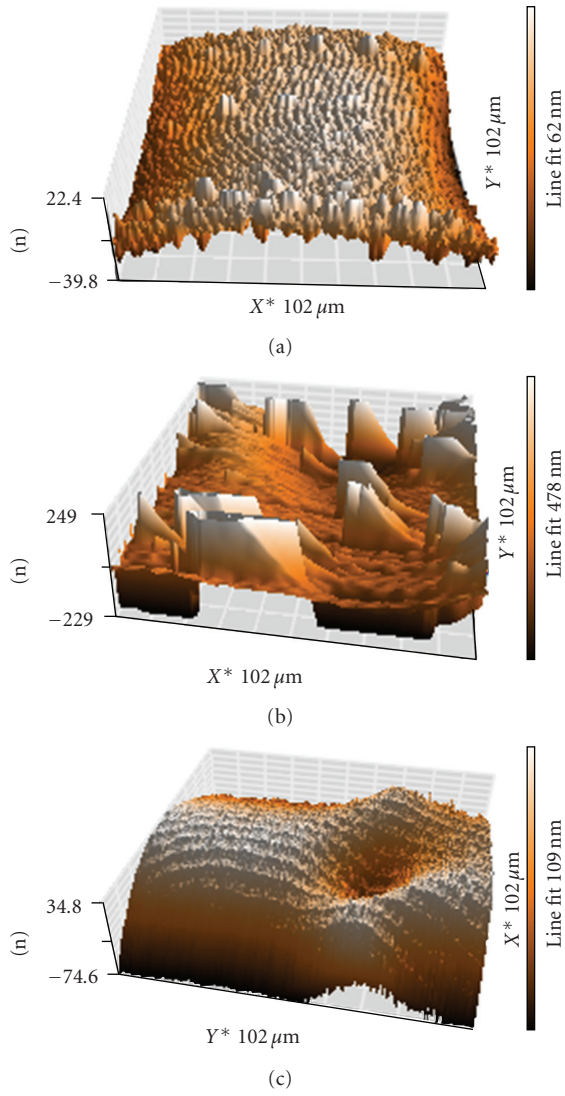

FIGURE 5: AFM topography of (a) polished copper surface without any treatment, (b) solution-treated surface without inhibitor in 0.5-M HCl, and (c) with 10-mM ATA in 0.5-M HCl.

4. Conclusion

Corrosion behavior of copper was studied in 0.5-M HCl solution with and without ATA as corrosion inhibitor. Polarization plots were obtained with different concentrations of ATA. The corrosion inhibition efficiency of up to 74% was achieved at the 10-mM concentration of ATA. Impedance spectra of the inhibited and uninhibited solutions were characterized by two slightly distorted capacity behaviours, one at high frequency and the other at low frequency. EIS experiments also showed an increase in charge transfer resistance in presence of the inhibitor. The characteristics of the Cu dissolution in the test solution were studied with RRDE voltammetric technique. Cu dissolves both in the form of Cu(I) and Cu(II) soluble species. The proportion of Cu(I) species decreased at the higher anodic polarization. Analysis of electrochemical noise data indicated the lowering of

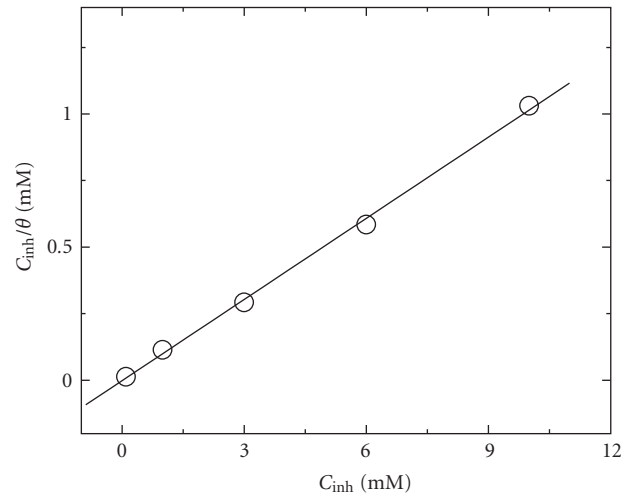

FIGURE 6: Plot of C_{inh}/θ versus C_{inh} following Langmuir adsorption isotherm.

localized corrosion in presence of the inhibitor. Adsorption of the inhibitor followed Langmuir adsorption isotherm with adsorption coefficient of $1.2 \times 10^6\ M^{-1}$. Standard free energy change of adsorption of $-54.3\ kJ\ mol^{-1}$ indicated that the chemical interaction of the inhibitor with the metal surface, which could be through the interaction of the π-electron cloud of the aromatic ring and also the free electron pair on the nitrogen atom with metal ions at the surface.

References

[1] G. W. Poling, "Reflection infra-red studies of films formed by benzotriazole on Cu," *Corrosion Science*, vol. 10, no. 5, pp. 359–370, 1970.

[2] T. Notoya and G. W. Poling, "Topographies of Thick Cu-Benzotriazolate Films on Copper," *Corrosion*, vol. 32, no. 6, pp. 216–223, 1976.

[3] A. Frignani, L. Tommesani, G. Brunoro, C. Monticelli, and M. Fogagnolo, "Influence of the alkyl chain on the protective effects of 1,2,3-benzotriazole towards copper corrosion. Part I: inhibition of the anodic and cathodic reactions," *Corrosion Science*, vol. 41, no. 6, pp. 1205–1215, 1999.

[4] P. R. P. Rodrigues, I. V. Aoki, A. H. P. De Andrade, E. De Oliveira, and S. M. L. Agostinho, "Effect of benzotriazole on electrochemical and corrosion behaviour of type 304 stainless steel in 2M sulphuric acid solution," *British Corrosion Journal*, vol. 31, no. 4, pp. 305–308, 1996.

[5] P. R. P. Rodrigues, J. O. Zerbino, and S. M. L. Agostinho, "Voltammetric and ellipsometric studies of films formed on 304 stainless steel in sulphuric acid solution without and with benzotriazole," *Materials Science Forum*, vol. 289, no. 2, pp. 1299–1310, 1998.

[6] F. El-Taib Heakal and S. Haruyama, "Impedance studies of the inhibitive effect of benzotriazole on the corrosion of copper in sodium chloride medium," *Corrosion Science*, vol. 20, no. 7, pp. 887–898, 1980.

[7] M. R. G. de Chialvo, R. C. Salvarezza, D. Vasquez Moll, and A. J. Arvia, "Kinetics of passivation and pitting corrosion of polycrystalline copper in borate buffer solutions containing

sodium chloride," *Electrochimica Acta*, vol. 30, no. 11, pp. 1501–1511, 1985.

[8] F. Bentiss, M. Bouanis, B. Mernari, M. Traisnel, H. Vezin, and M. Lagrenée, "Understanding the adsorption of 4H-1,2,4-triazole derivatives on mild steel surface in molar hydrochloric acid," *Applied Surface Science*, vol. 253, no. 7, pp. 3696–3704, 2007.

[9] W. Li, Q. He, C. Pei, and B. Hou, "Experimental and theoretical investigation of the adsorption behaviour of new triazole derivatives as inhibitors for mild steel corrosion in acid media," *Electrochimica Acta*, vol. 52, no. 22, pp. 6386–6394, 2007.

[10] L. Wang, "Inhibition of mild steel corrosion in phosphoric acid solution by triazole derivatives," *Corrosion Science*, vol. 48, no. 3, pp. 608–616, 2006.

[11] T. Kosec, I. Milošev, and B. Pihlar, "Benzotriazole as an inhibitor of brass corrosion in chloride solution," *Applied Surface Science*, vol. 253, no. 22, pp. 8863–8873, 2007.

[12] V. Otieno-Alego, G. A. Hope, T. Notoya, and D. P. Schweinsberg, "An electrochemical and sers study of the effect of 1 -[N,N-bis-(hydroxyethyl) aminomethyl]-benzotriazole on the acid corrosion and dezincification of 60/40 brass," *Corrosion Science*, vol. 38, no. 2, pp. 213–223, 1996.

[13] D. P. Schweinsberg, S. E. Bottle, V. Otieno-Alego, and T. Notoya, "A near-infrared FT-Raman (SERS) and electrochemical study of the synergistic effect of 1-[(1′,2′-dicarboxy)ethyl]-benzotriazole and KI on the dissolution of copper in aerated sulfuric acid," *Journal of Applied Electrochemistry*, vol. 27, no. 2, pp. 161–168, 1997.

[14] H. Otmacic, J. Telegdi, K. Papp, and E. Stupnisek-lisac, "Protective properties of an inhibitor layer formed on copper in neutral chloride solution," *Journal of Applied Electrochemistry*, vol. 34, no. 5, pp. 545–550, 2004.

[15] J. Bartley, N. Huynh, S. E. Bottle, H. Flitt, T. Notoya, and D. P. Schweinsberg, "Computer simulation of the corrosion inhibition of copper in acidic solution by alkyl esters of 5-carboxybenzotriazole," *Corrosion Science*, vol. 45, no. 1, pp. 81–96, 2003.

[16] H. Ma, S. Chen, L. Niu, S. Zhao, S. Li, and D. Li, "Inhibition of copper corrosion by several Schiff bases in aerated halide solutions," *Journal of Applied Electrochemistry*, vol. 32, no. 1, pp. 65–72, 2002.

[17] L. J. Berchmans, V. Sivan, and S. V. K. Iyer, "Studies on triazole derivatives as inhibitors for the corrosion of muntz metal in acidic and neutral solutions," *Materials Chemistry and Physics*, vol. 98, no. 2-3, pp. 395–400, 2006.

[18] D.-Q. Zhang, L.-X. Gao, G.-D. Zhou, and K. Y. Lee, "Undecyl substitution in imidazole and its action on corrosion inhibition of copper in aerated acidic chloride media," *Journal of Applied Electrochemistry*, vol. 38, no. 1, pp. 71–76, 2008.

[19] A. K. Satpati, M. M. Palrecha, and R. I. Sundaresan, "Electrochemical study of the mechanism of interaction of 1,2,3-benzotriazole on SS304 surface in HCl medium," *Indian Journal of Chemical Technology*, vol. 15, no. 2, pp. 163–167, 2008.

[20] A. K. Satpati and P. V. Ravindran, "Electrochemical study of the inhibition of corrosion of stainless steel by 1,2,3-benzotriazole in acidic media," *Materials Chemistry and Physics*, vol. 109, no. 2-3, pp. 352–359, 2008.

[21] B. Trachli, M. Keddam, H. Takenouti, and A. Srhiri, "Protective effect of electropolymerized 3-amino 1,2,4-triazole towards corrosion of copper in 0.5 M NaCl," *Corrosion Science*, vol. 44, no. 5, pp. 997–1008, 2002.

[22] Z. Mountassir and A. Srhiri, "Electrochemical behaviour of Cu-40Zn in 3% NaCl solution polluted by sulphides: effect of aminotriazole," *Corrosion Science*, vol. 49, no. 3, pp. 1350–1361, 2007.

[23] M. Itagaki, M. Tagaki, and K. Watanabe, "Study of dissolution mechanisms of copper in perchloric acid solution containing NaCl by channel flow double electrode and electrochemical quartz crystal microbalance," *Corrosion Science*, vol. 38, no. 7, pp. 1109–1125, 1996.

[24] D. Tromans and J. C. Silva, "Behavior of copper in acidic sulfate solution: comparison with acidic chloride," *Corrosion*, vol. 53, no. 3, pp. 171–178, 1997.

[25] C. Deslouis, B. Tribollet, G. Mengoli, and M. M. Musiani, "Electrochemical behaviour of copper in neutral aerated chloride solution. I: steady-state investigation," *Journal of Applied Electrochemistry*, vol. 18, no. 3, pp. 374–383, 1988.

[26] J. J. Shim and J. G. Kim, "Copper corrosion in potable water distribution systems: influence of copper products on the corrosion behavior," *Materials Letters*, vol. 58, no. 14, pp. 2002–2006, 2004.

[27] M. Xu and H. D. Dewald, "Impedance studies of copper foil and graphite-coated copper foil electrodes in lithium-ion battery electrolyte," *Electrochimica Acta*, vol. 50, no. 27, pp. 5473–5478, 2005.

[28] Y. Feng, W. K. Teo, K. S. Siow, K. L. Tan, and A. K. Hsieh, "The corrosion behaviour of copper in neutral tap water. Part I: corrosion mechanisms," *Corrosion Science*, vol. 38, no. 3, pp. 369–385, 1996.

[29] K. Jüttner, "Electrochemical impedance spectroscopy (EIS) of corrosion processes on inhomogeneous surfaces," *Electrochimica Acta*, vol. 35, no. 10, pp. 1501–1508, 1990.

[30] E. McCafferty and N. Hackerman, "Double layer capacitance of iron and corrosion inhibition with polymethylene diamines," *Journal of the Electrochemical Society*, vol. 119, pp. 146–154, 1972.

[31] R. Macdonald and D. R. Franceschetti, "The electrical analogs of physical and chemical processes," in *Impedance Spectroscopy*, J. R. Macdonald, Ed., p. 39, John Wiley & Sons, New York, NY, USA, 1987.

[32] S. F. Mertens, C. Xhoffer, B. C. De Cooman, and E. Temmerman, "Short-term deterioration of polymer-coated 55% Al-Zn—part 1: behavior of thin polymer films," *Corrosion*, vol. 53, no. 5, pp. 381–387, 1997.

[33] A. Popova and M. Christov, "Evaluation of impedance measurements on mild steel corrosion in acid media in the presence of heterocyclic compounds," *Corrosion Science*, vol. 48, no. 10, pp. 3208–3221, 2006.

[34] H. Gerengi, K. Darowicki, G. Bereket, and P. Slepski, "Evaluation of corrosion inhibition of brass-118 in artificial seawater by benzotriazole using dynamic EIS," *Corrosion Science*, vol. 51, no. 11, pp. 2573–2579, 2009.

[35] R. S. Cooper, "Schlieren studies of concentration gradients at a Cu—HClAnode," *Journal of the Electrochemical Society*, vol. 105, pp. 506–512, 1958.

[36] A. J. Calandra, N. R. de Tacconi, R. Pereiro, and A. J. Arvia, "Potentiodynamic current/potential relations for film formation under OHMIC resistance control," *Electrochimica Acta*, vol. 19, no. 12, pp. 901–905, 1974.

[37] H. P. Lee, K. Nobe, and A. J. Pearlstein, "Film formation and current oscillations in the electrodissolution of Cu in acidic chloride media. Part I: experimental studies," *Journal of the Electrochemical Society*, vol. 132, no. 5, pp. 1031–1037, 1985.

[38] A. J. Pearlstein, H. P. Lee, and K. Nobe, "Film formation and current oscillations in the electrodissolution of copper in

acidic chloride media. II: mathematical model," *Journal of the Electrochemical Society*, vol. 132, no. 9, pp. 2159–2165, 1985.

[39] S. L. F. A. Costa, S. M. L. Agostinho, and K. Nobe, "Rotating ring-disk electrode studies of Cu-Zn alloy electrodissolution in M HCl effect of benzotriazole," *Journal of the Electrochemical Society*, vol. 140, no. 12, pp. 3483–3488, 1993.

[40] E. Geler and D. S. Azambuja, "Corrosion inhibition of copper in chloride solutions by pyrazole," *Corrosion Science*, vol. 42, no. 4, pp. 631–643, 2000.

[41] C. Gouveia-Caridade, M. I. S. Pereira, and C. M. A. Brett, "Electrochemical noise and impedance study of aluminium in weakly acid chloride solution," *Electrochimica Acta*, vol. 49, no. 5, pp. 785–793, 2004.

[42] F. Mansfeld and H. Xiao, "Electrochemical noise analysis of iron exposed to NaCl solutions of different corrosivity," *Journal of the Electrochemical Society*, vol. 140, no. 8, pp. 2205–2209, 1993.

[43] U. Bertocci, C. Gobrielli, F. Huet, and M. Keddam, "Noise resistance applied to corrosion measurements: I. Theoretical analysis," *Journal of the Electrochemical Society*, vol. 144, no. 1, pp. 31–37, 1997.

[44] D. J. Mills, G. P. Bierwagen, B. Skerry, and D. Tallman, "Investigation of anticorrosive coatings by the electrochemical noise method," *Materials Performance*, vol. 34, no. 5, pp. 33–38, 1995.

[45] U. Bertocci, C. Gabrielli, F. Huet, M. Keddam, and P. Rousseau, "Noise resistance applied to corrosion measurements: II. Experimental tests," *Journal of the Electrochemical Society*, vol. 144, no. 1, pp. 37–43, 1997.

[46] R. A. Cottis, M. A. Al-Awadhi, H. Al-Mazeedi, and S. Turgoose, "Testing and analyzing metastable pitting corrosion," *Electrochimica Acta*, vol. 46, no. 24-25, pp. 3699–3703, 2001.